organic compounds

Hydrogen bonding in the bromide salts of 4-aminobenzoic acid and 4-amino-acetophenone

Dominik Cinčić and Branko Kaitner*

Department of Chemistry, Laboratory of General and Inorganic Chemistry, Faculty of Science, University of Zagreb, Horvatovac 102a, HR-10000 Zagreb, Croatia
Correspondence e-mail: kaitner@chem.pmf.hr

In the title compounds, 4-carboxyanilinium bromide, C_7H_8-$NO_2^+ \cdot Br^-$, (I), and 4-acetylanilinium bromide, $C_8H_{10}NO^+ \cdot Br^-$, (II), each asymmetric unit contains a discrete cation with a protonated amino group and a halide anion. Both crystal structures are characterized by two-dimensional hydrogen-bonded networks. The ions in (I) are connected via N—H···Br, N—H···O and O—H···Br hydrogen bonds, with three characteristic graph-set motifs, viz. $C(8)$, $C_2^1(4)$ and $R_3^2(8)$. The centrosymmetric hydrogen-bonded $R_2^2(8)$ dimer motif characteristic of carboxylic acids is absent. The ions in (II) are connected via N—H···Br and N—H···O hydrogen bonds, with two characteristic graph-set motifs, viz. $C(8)$ and $R_4^2(8)$. The significance of this study lies in its illustration of the differences between the supramolecular aggregations in two similar compounds. The presence of the methyl group in (II) at the site corresponding to the hydroxyl group in (I) results in a significantly different hydrogen-bonding arrangement.

Comment

The synthesis of salts provides pharmaceutical scientists with the opportunity to modify the physicochemical properties of active pharmaceutical ingredients (APIs) or potential drug substances. The salt form can influence the range of properties, such as aqueous solubility, melting point, hygroscopicity, dissolution rate and crystallinity (Gould, 1986; Bastin et al., 2000). The title compounds, viz. 4-carboxyanilinium bromide, (I), and 4-acetylanilinium bromide, (II), were originally investigated during salt screening of aromatic monoamines and represent a part of our research into intermolecular interactions in hydrogen-bonded ionic crystals of acid salts (Cinčić & Kaitner, 2007, 2008). 4-Aminobenzoic (PABA) acid is widely known as bacterial vitamin H and as one of the components of the vitamin B complex. It is also an important biological molecule, acting as an antagonist to the action of sulfanilamide drugs in competition for essential growth metabolites, as well as being an essential bacterial cofactor

involved in the synthesis of folic acid (Woods, 1940; Brown et al., 1961). 4-Aminoacetophenone has been less extensively studied than PABA, but its derivatives have been widely studied. In the present study, we chose 4-aminoacetophenone as another compound containing both amino and carbonyl groups. The presence of the methyl group in (II) at the site corresponding to the hydroxyl group in (I) results in different crystal packing and hydrogen-bonding arrangements, as described below.
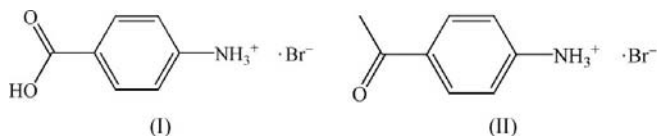

In the title compounds, (I) and (II), the bond lengths and angles are all normal for their types (Allen et al., 1987). The asymmetric unit of each of (I) and (II) contains a halide anion and a discrete cation with a protonated amino group (Figs. 1 and 2). Compound (I) is isostructural with the analogous chloride salt (Colapietro et al., 1980). However, that study was concerned primarily with the detailed geometry of the aryl ring in the presence of two substituents with markedly different electron donor/acceptor properties, whereas the hydrogen bonding was discussed only briefly. Moreover, the precision of the present study is considerably higher, with a lower R index, despite a considerably higher data-to-parameter ratio (15.8 versus 12.7) and with s.u. values on the ring bond angles ca 0.1 times those reported previously. Because of the difference in anionic radii, the volume of the unit cell in (I) is about 37 $Å^3$ larger than that of the chloride salt. Compound
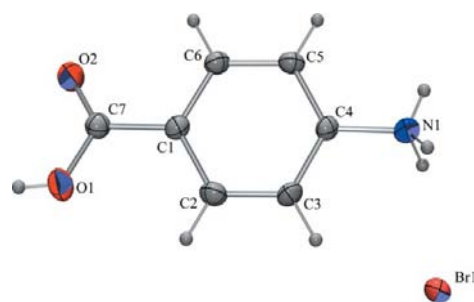
Figure 1
The asymmetric unit of (I), showing the atom-numbering scheme. Displacement ellipsoids are drawn at the 30% probability level and H atoms are shown as small spheres of arbitrary radii.
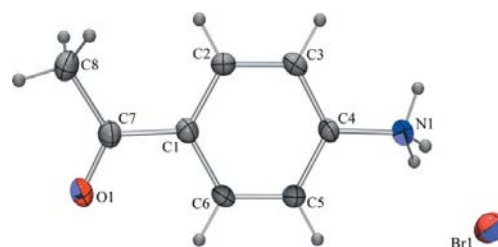
Figure 2
The asymmetric unit of (II), showing the atom-numbering scheme. Displacement ellipsoids are drawn at the 30% probability level and H atoms are shown as small spheres of arbitrary radii.
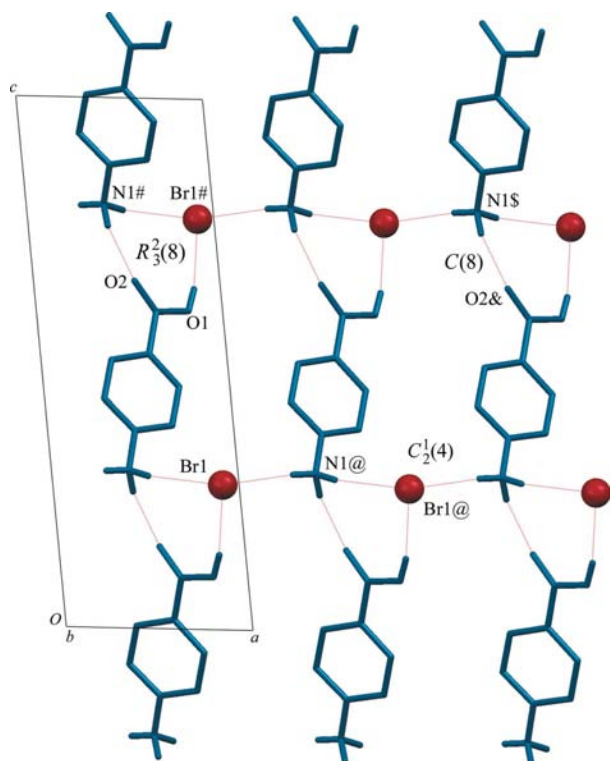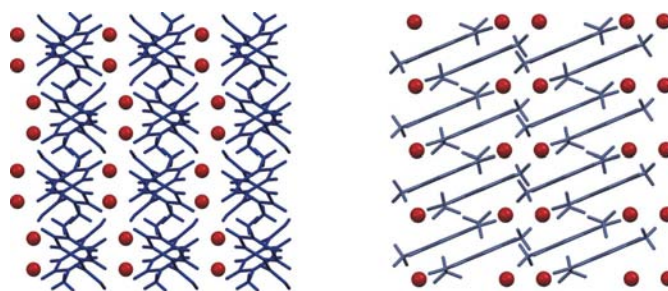
Figure 3
A view of the two-dimensional hydrogen-bonded network of (I) parallel to the (010) plane, showing the aggregation of three hydrogen-bonding motifs, *viz.* $C(8)$, $C_2^1(4)$ and $R_3^2(8)$. Hydrogen bonds are drawn as dotted lines and C-bound H atoms have been omitted. Atoms marked with an ampersand (&), an 'at' sign (@), a hash symbol (#) or a dollar sign ($) are at the symmetry positions $(2 + x, y, z)$, $(1 + x, y, z)$, $(x, \frac{3}{2} - y, \frac{1}{2} + z)$, $(2 + x, \frac{3}{2} - y, \frac{1}{2} + z)$, respectively.

(II) is not isostructural with that of the chloride analogue, which crystallizes as a monohydrate (Ersanlı *et al.*, 2004).

In (I), the ions are connected into a two-dimensional hydrogen-bonded network parallel to the (010) plane *via* N—H···Br, N—H···O and O—H···Br hydrogen bonds. There are no centrosymmetric hydrogen-bonded dimers between the carboxylic acid groups of adjacent 4-carboxyanilinium cations, which is a characteristic feature found in most salts of 3- and 4-aminobenzoic acid (Cambridge Structural Database, Version 5.29; Allen, 2002). The carbonyl O atom participates in hydrogen bonding with a neighbouring cation through an N—H···O hydrogen bond. This interaction links the glide-plane-related cations into zigzag chains which run parallel to the [001] direction and which can be described by a graph-set motif of $C(8)$ (Bernstein *et al.*, 1995) (Fig. 3). The carboxyl H atom participates in hydrogen bonding with a neighbouring anion through an O—H···Br hydrogen bond. All ammonium H atoms are involved in hydrogen bonds with two different Br− ions and with the carbonyl O atom of a neighbouring cation, while each anion accepts three hydrogen bonds. The two ammonium–anion interactions link the anions and cations in an alternating fashion into extended chains along the [100] direction which can be described by a graph-set motif of $C_2^1(4)$. The noncentrosymmetric hydrogen-bonded rings formed by adjacent 4-carboxyanilinium cations and one halide anion can

Figure 4
Packing diagrams of (I) (left) and (II) (right), viewed along the *c* and *b* axes, respectively.
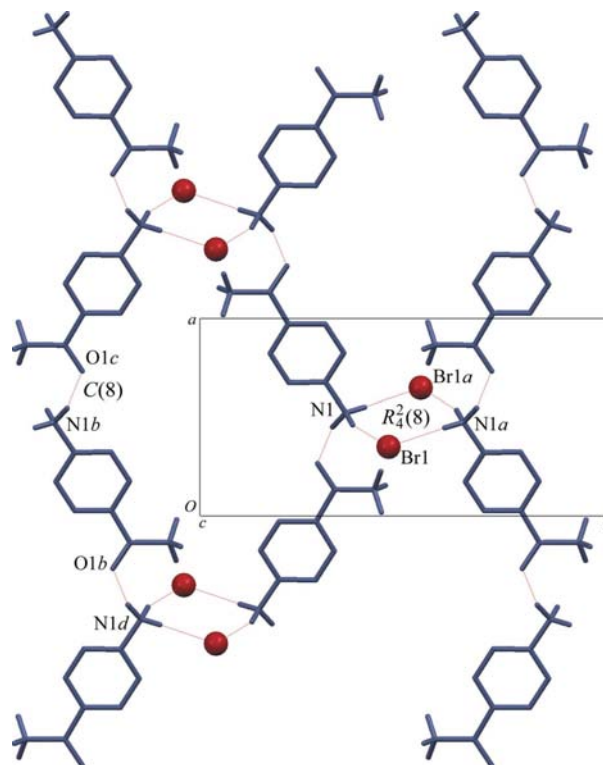
Figure 5
A view of the two-dimensional hydrogen-bonded network of (II) parallel to the ($\bar{1}02$) plane, showing the aggregation of three hydrogen-bonding motifs, *viz.* $C(8)$ and $R_4^2(8)$. Hydrogen bonds are drawn as dotted lines and aromatic C-bound H atoms have been omitted. Atoms marked with the suffixes *a, b, c* and *d* are at the symmetry positions $(1 - x, 1 - y, 1 - z)$, $(1 - x, -y, 1 - z)$, $(2 - x, y - \frac{1}{2}, \frac{3}{2} - z)$ and $(-x, y - \frac{1}{2}, \frac{1}{2} - z)$, respectively.

be described by the graph-set motif $R_3^2(8)$. The aggregation of ring and chain motifs results in an overall two-dimensional hydrogen-bonded sheet-like structure (Fig. 3). Adjacent sheets are stacked in the [010] direction to give a three-dimensional framework, where the interplanar distance between the aromatic rings of each sheet is *ca* 3.38 Å. The interplanar distance between aromatic rings of each sheet in the isostructural chloride salt is, unexpectedly, almost the same at *ca* 3.33 Å, and adjacent sheets are further linked *via* inter-layer N—H···Cl interactions.

Because of the different functional group on atom C7 in (I) and (II), the supramolecular structures of the two compounds differ. Fig. 4 clearly compares the packing arrangement of both compounds. The ions of (II) are connected into a two-

dimensional hydrogen-bonded network, this time parallel to the $(\bar{1}02)$ plane, *via* N—H···Br and N—H···O hydrogen bonds (Table 2). As in (I), all ammonium H atoms in (II) are involved in hydrogen bonds with two different Br$^-$ ions and with the carbonyl O atom of a neighbouring cation, while each anion accepts two hydrogen bonds. Also as in (I), the carbonyl O atom participates in hydrogen bonding with a neighbouring cation through an N—H···O hydrogen bond. This interaction links the glide-plane-related cations into zigzag chains which run parallel to the [001] direction and which can be described by a graph-set motif of $C(8)$ (Fig. 5). The centrosymmetric hydrogen-bonded rings formed by adjacent cations in the chains can be described by the graph-set motif $R_4^2(8)$. The aggregation of ring and chain motifs in (II) also leads to a two-dimensional hydrogen-bonded sheet-like structure (Fig. 5). Adjacent sheets are stacked in the $[\bar{1}02]$ direction to give a three-dimensional framework, where weak interlayer C—H···Br interactions are present [C6···Br1$(x + 1, y, z)$ = 3.854 (3) Å and C8···Br1$(x + 1, -y + \frac{1}{2}, z - \frac{1}{2})$ = 3.809 (4) Å]. No intermolecular π–π interactions are evident in either crystal structure. The shortest centroid-to-centroid distances in (I) and (II) are *ca* 4.06 and 3.86 Å, respectively.

Experimental

For the preparation of (I), 3-aminobenzoic acid (100 mg, 0,73 mmol) was dissolved in hot ethanol (2 ml). The resulting clear solution was added to aqueous hydrobromic acid (2 ml, 2 M) and cooled to room temperature. Colourless crystals of (I) were grown by slow evaporation. For the preparation of (II), 4-aminoacetophenone (100 mg, 0.74 mmol) was dissolved in a hot mixture of ethanol and propan-2-ol (3 ml, 2:1 *v/v*). The resulting clear solution was added to hydrobromic acid (1 ml, 2 M) and cooled to room temperature. Colourless crystals of (II) were grown by slow evaporation. Crystals of (I) and (II) were collected by vacuum filtration, washed with cold acetone and dried in air. Under a nitrogen atmosphere, (I) and (II) melt at 524 and 472 K, respectively.

Compound (I)

Crystal data

$C_7H_8NO_2{}^+\cdot Br^-$	$V = 819.1\ (2)$ Å^3
$M_r = 218.05$	$Z = 4$
Monoclinic, $P2_1/c$	Mo $K\alpha$ radiation
$a = 5.8209\ (9)$ Å	$\mu = 4.97$ mm^{-1}
$b = 8.5101\ (11)$ Å	$T = 295$ K
$c = 16.648\ (3)$ Å	$0.50 \times 0.11 \times 0.11$ mm
$\beta = 96.660\ (13)°$	

Data collection

Oxford Diffraction Xcalibur CCD diffractometer	7029 measured reflections
	1787 independent reflections
Absorption correction: analytical (Alcock, 1970)	1573 reflections with $I > 2\sigma(I)$
$T_{\min} = 0.294$, $T_{\max} = 0.619$	$R_{\text{int}} = 0.023$

Refinement

$R[F^2 > 2\sigma(F^2)] = 0.030$	H atoms treated by a mixture of independent and constrained refinement
$wR(F^2) = 0.093$	
$S = 1.16$	
1787 reflections	$\Delta\rho_{\max} = 0.61$ e Å^{-3}
113 parameters	$\Delta\rho_{\min} = -0.60$ e Å^{-3}

Table 1
Hydrogen-bond geometry (Å, °) for (I).

D—H···A	D—H	H···A	D···A	D—H···A
N1—H1A···Br1	0.84 (6)	2.55 (5)	3.343 (3)	159 (5)
O1—H1···Br1$^{\text{i}}$	0.78	2.47	3.238 (2)	170
N1—H1B···O2$^{\text{ii}}$	0.83 (5)	1.99 (5)	2.781 (4)	158 (5)
N1—H1C···Br1$^{\text{iii}}$	0.81 (4)	2.48 (4)	3.291 (3)	173 (4)

Symmetry codes: (i) $x, -y + \frac{3}{2}, z + \frac{1}{2}$; (ii) $x, -y + \frac{3}{2}, z - \frac{1}{2}$; (iii) $x - 1, y, z$.

Table 2
Hydrogen-bond geometry (Å, °) for (II).

D—H···A	D—H	H···A	D···A	D—H···A
N1—H1B···Br1	0.86 (4)	2.41 (4)	3.236 (3)	162 (4)
N1—H1A···Br1$^{\text{i}}$	0.88 (4)	2.41 (4)	3.278 (3)	168 (3)
N1—H1C···O1$^{\text{ii}}$	0.90 (4)	1.89 (4)	2.766 (4)	163 (4)

Symmetry codes: (i) $-x + 1, -y + 1, -z + 1$; (ii) $x - 1, -y + \frac{1}{2}, z - \frac{1}{2}$.

Compound (II)

Crystal data

$C_8H_{10}NO^+\cdot Br^-$	$V = 883.5\ (2)$ Å^3
$M_r = 216.08$	$Z = 4$
Monoclinic, $P2_1/c$	Mo $K\alpha$ radiation
$a = 7.4423\ (8)$ Å	$\mu = 4.59$ mm^{-1}
$b = 15.4529\ (10)$ Å	$T = 295$ K
$c = 7.6833\ (14)$ Å	$0.41 \times 0.10 \times 0.09$ mm
$\beta = 90.828\ (8)°$	

Data collection

Oxford Diffraction Xcalibur CCD diffractometer	12753 measured reflections
	1904 independent reflections
Absorption correction: analytical (Alcock, 1970)	1710 reflections with $I > 2\sigma(I)$
$T_{\min} = 0.346$, $T_{\max} = 0.701$	$R_{\text{int}} = 0.061$

Refinement

$R[F^2 > 2\sigma(F^2)] = 0.039$	H atoms treated by a mixture of independent and constrained refinement
$wR(F^2) = 0.127$	
$S = 1.23$	
1904 reflections	$\Delta\rho_{\max} = 0.78$ e Å^{-3}
114 parameters	$\Delta\rho_{\min} = -0.62$ e Å^{-3}

All N- and O-bound H atoms in (I) and all N-bound H atoms in (II) were located in difference Fourier maps. For both compounds, the positions and isotropic displacement parameters of the N-bound H atoms were refined [N—H = 0.81 (4)–0.90 (4) Å]. The hydroxyl H atom in (I) was fixed at the position found from the difference map (O—H = 0.78 Å). H atoms bonded to C atoms were treated as riding, with C—H = 0.93 (aromatic) or 0.96 Å (methyl), and with $U_{\text{iso}}(\text{H}) = kU_{\text{eq}}(\text{C})$, where $k = 1.5$ for methyl and 1.2 for aromatic H atoms.

For both compounds, data collection: *CrysAlis CCD* (Oxford Diffraction, 2003); cell refinement: *CrysAlis RED* (Oxford Diffraction, 2003); data reduction: *CrysAlis RED*; program(s) used to solve structure: *SHELXS97* (Sheldrick, 2008); program(s) used to refine structure: *SHELXL97* (Sheldrick, 2008); molecular graphics: *ORTEP-3* (Farrugia, 1997); software used to prepare material for publication: *WinGX* (Farrugia, 1999), *PARST97* (Nardelli, 1995), *Mercury* (Version 1.4; Macrae *et al.*, 2006) and *POV-RAY* (Persistence of Vision Team, 2004).

Supplementary data for this paper are available from the IUCr electronic archives (Reference: GD3202). Services for accessing these data are described at the back of the journal.

References

Alcock, N. W. (1970). *Crystallographic Computing*, edited by F. R. Ahmed, S. R. Hall & C. P. Huber, p. 271. Copenhagen: Munksgaard.

Allen, F. H. (2002). *Acta Cryst.* B**58**, 380–388.

Allen, F. H., Kennard, O., Watson, D. G., Brammer, L., Orpen, A. G. & Taylor, R. (1987). *J. Chem. Soc. Perkin Trans. 2*, pp. S1–19.

Bastin, R. J., Bowker, M. J. & Slater, B. J. (2000). *Org. Process Res. Dev.* **4**, 427–435.

Bernstein, J., Davis, R. E., Shimoni, L. & Chang, N.-L. (1995). *Angew. Chem. Int. Ed. Engl.* **34**, 1555–1573.

Brown, G. M., Weisman, R. A. & Molnar, D. A. (1961). *J. Biol. Chem.* **236**, 2534–2543.

Cinčić, D. & Kaitner, B. (2007). *Acta Cryst.* E**63**, o3873.

Cinčić, D. & Kaitner, B. (2008). *Acta Cryst.* C**64**, o101–o104.

Colapietro, M., Domenicano, A. & Portalone, G. (1980). *Acta Cryst.* B**36**, 354–358.

Ersanlı, C. C., Odabaşoğlu, M., Albayrak, Ç., Büyükgüngör, O. & Erdönmez, A. (2004). *Acta Cryst.* E**60**, o397–o398.

Farrugia, L. J. (1997). *J. Appl. Cryst.* **30**, 565.

Farrugia, L. J. (1999). *J. Appl. Cryst.* **32**, 837–838.

Gould, P. L. (1986). *Int. J. Pharm.* **33**, 201–217.

Macrae, C. F., Edgington, P. R., McCabe, P., Pidcock, E., Shields, G. P., Taylor, R., Towler, M. & van de Streek, J. (2006). *J. Appl. Cryst.* **39**, 453–457.

Nardelli, M. (1995). *J. Appl. Cryst.* **28**, 659.

Oxford Diffraction (2003). *CrysAlis CCD* and *CrysAlis RED*. Versions 1.170. Oxford Diffraction Ltd, Wrocław, Poland.

Persistence of Vision Team (2004). *POV-RAY*. Version 3.6. Persistence of Vision Raytracer Pty Ltd, Victoria, Australia. URL: http://www.povray.org/.

Sheldrick, G. M. (2008). *Acta Cryst.* A**64**, 112–122.

Woods, D. D. (1940). *Br. J. Exp. Pathol.* **21**, 74–90.